TEMPERATURE DEPENDENCES IN THE O + OH → O_2 + H REACTION. QUASICLASSICAL TRAJECTORY CALCULATION

Viliam KLIMO[a], Martina BITTERÉROVÁ[b], Stanislav BISKUPIČ[b], Ján URBAN[a] and Miroslav MICOV[a]

[a] *Polymer Institute, Slovak Academy of Sciences, 842 36 Bratislava, The Slovak Republic*

[b] *Department of Physical Chemistry, Slovak Technical University, 812 37 Bratislava, The Slovak Republic*

Received December 20, 1991
Accepted April 4, 1992

The reaction O + OH → O_2 + H in conditions of combustion of hydrocarbons and polymers was modelled by using the method of quasiclassical trajectories. The potential energy surface was determined by the multiconfiguration interaction method and fitted with the analytical form of the extended LEPS function. Attention was paid to the mean values of the vibrational and rotational quantum numbers of O_2 molecules and their temperature dependence. The temperature dependence of the mean lifetime of the OOH collision complex was also examined. The calculated rate constants were analyzed and compared with the experimental data over the temperature region of the combustion processes.

The reaction O + OH → O_2 + H occurs mainly on the ground $^2A''$ potential energy surface and proceeds via the vibrationally or rotationally excited collision complex OOH*.

$$O\ (^3P) + OH\ (^2\Pi) \rightarrow OOH^*\ (X\ ^2A'') \rightarrow O_2\ (^3\Sigma_g^-) + H\ (^2S) \qquad (A)$$

This reaction is of high importance in the process of combustion of hydrocarbons and polymers, which it slows down appreciably[1] because it is the reverse reaction to the branching reaction H + O_2 → OH + O. Model calculations revealed[1] that it also slows down the flame propagation velocity. The reaction also plays a major role at extremely low temperatures in the interstellar space where its rate constant is substantially higher than as was expected[2] and so it can be the principal reaction responsible for the loss of OH radicals in interstellar clouds. The third field where the reaction in question is significant is in the Earth's atmosphere where it is involved in the mechanism of the global distribution of ozone[3]. The collision complex can be well stabilized under favourable conditions, and the OOH radical formed then affects significantly the chemical processes in various fields of radical chemistry[4]. For these reasons the reaction (*A*) has received interest with respect to its rate constant, which has been studied theoretically[5 – 10] as well as experimentally[11 – 13].

In the processes of combustion of hydrocarbons and in the gas envelope of burning polymers where reaction (*A*) proceeds, it is very important to investigate the high-temperature rate constant and its temperature dependence. The temperature region concerned is from 500 to 2 000 K (refs[14,15]). In addition to the temperature dependence of the rate constant, quasiclassical trajectory (QCT) calculations provide other dynamic characteristics which are relevant with respect to the effect on the overall combustion mechanism. Molecular oxygen $O_2(^3\Sigma_g^-)$, which is a reaction product, can occur in an excited rotational-vibrational state (can be rotationally or vibrationally "hot"). This will affect its reactivity in all reactions of the reaction mechanism in which it is involved. For this reason we investigated the mean rotational quantum number $\bar{j}'$ and the mean vibrational quantum number $\bar{v}'$ of the O_2 molecule and their temperature dependences. We also examined the mean lifetime $\bar{t}$ of the OOH ($X\ ^2A''$) collision complex and its temperature dependence. This quantity correlates with the probability of stabilization of the OOH radical by collision with a third particle and so affects the opportunity for the OOH radical to get involved in the combustion process.

The first part of this paper gives an overview of the recent calculation of the hypersurface for reaction (*A*) and describes the base and the MC SCF method used. It also contains a description of the ELEPS hypersurface and its parameters, by means of which the *ab initio* points were fitted. The results of calculation are presented for the equilibrium geometry and the minimum energy in the limits of the input (O + OH) and output (O_2 + H) channels as well as in the equilibrium region of the OOH collision complex. In the second part, the above dynamic characteristics ($\bar{j}', \bar{v}', \bar{t}'$) and their temperature dependences are presented and discussed. The last part deals with the rate constant of reaction (*A*) and its temperature dependence. The temperature dependence of that part of the rate constant associated with the fine splitting of the reactant levels is discussed. The QCT dependence of the rate constant over the 500 – 2 000 K region is compared with recent experimental results.

Potential Energy Surface

The potential energy surface (PES) of the OOH system has been studied by several authors at the *ab initio* level[16 – 19], whereas Graff and coworkers[10] used the multipole expansion type of the Hamiltonian extended with the spin–orbit interaction part. This work provides *ab initio* MC SCF calculations based on the exponential operator method[21], implemented using the COLUMBUS program package[22,23]. The Gaussian basic set[24,25] employed consisted of the (9*s* 5*p* 1*d*) / [5*s* 3*p* 1*d*] base for the oxygen atom with an exponent of 0.9 for the *d*-orbital, and of the (5*s* 1*p*) / [3*s* 1*p*] base for the hydrogen atom with an exponent of 0.23 for the *p*-orbital. The active space in the MC SCF wave function was formed by the orbitals

$$\ldots\ (a_7')\ (a_{35}'')\ (a_8')\ (a_{36}'')\ \ldots,$$

based on which, nine configurations of the $^2A''$ symmetry were generated. These configuration functions of state, which represent the complete active space in the given set of orbitals, were used in all PES calculations without additional selection. The convergence criteria for the molecular orbitals and MC SCF expansion coefficients were chosen so that the total energy was calculated with a precision of 10^{-6} hartree. From the complete space of internuclear distances, 165 representative points were selected and the MC SFC energies were calculated for them. The equilibrium geometric parameters along with the equilibrium MC SCF energies are compared with experimental data[26,27] and with the MC SCF data by Melius and coworkers[17] in Table I. Except for the E_{min} value for the O_2 + H output channel, the data are in a good mutual agreement.

The representative *ab initio* PES points were used for fitting the parameters of the analytical representation of the PES in the form suggested by Wagner and coworkers[28]. The extended LEPS (ELEPS) analytical function of potential energy V as proposed by those authors is

$$V = \sum_{i=1}^{3} Q_i - (\sum_{i=1}^{3} \alpha_i^2 - \alpha_1 \alpha_2 - \alpha_1 \alpha_3 - \alpha_2 \alpha_3)^{1/2}, \qquad (1)$$

where the symbols Q_i and α_i can be written as

$$Q_i = D_i(a_i e_i^2 - b_i e_i)$$

$$a_i = D_i [(1 - a_i) e_i - (2 - b_i) e_i] \qquad (2)$$

$$e_i = \exp [-\beta_i (R_i - R_{ei})] .$$

TABLE I
Equilibrium geometric parameters and equilibrium MC SCF energies of the OOH ($X\ ^2A''$) system

System	R_{OO}, bohr	R_{OH}, bohr	O–O–H, deg	$-E_{min}$, hartree
O + OH	–	1.80[a]	–	150.2071[a]
	–	1.85[b]	–	150.2412[b]
	–	1.83[c]	–	–
OOH	2.65[a]	1.85[a]	105[a]	150.2562[a]
	2.58[b]	1.88[b]	104.2[b]	150.2998[b]
	2.51[d]	1.84[d]	104.0[d]	–
O_2 + H	2.19[a]	–	–	150.1366[a]
	2.33[b]	–	–	150.2181[b]
	2.28[c]	–	–	–

[a] This work; [b] ref.[17]; [c] ref.[26]; [d] ref.[27].

In the above equations, the i-th bond is associated with the dissociation energy D_i, spectroscopic constant β_i, equilibrium distance R_{ei} and fitting parameters a_i and b_i. Their actual values for the OOH system under study are given in Table II.

The ELEPS surface was represented by a contour line map of the potential energy in dependence on the R_{OO} and R_{OH} internuclear distances. The maps are shown in Fig. 1 for three O–O–H angles, viz. 60°, 99° and 150°. The map for 99° shows the region of the absolute minimum of the ELEPS surface – the OOH radical region. The overall

TABLE II
ELEPS surface parameters of the OOH system

System	D_e, hartree	β_e, bohr^{-1}	R_e, bohr	a	b
O–O	0.18441	1.4313	2.2819	2.4553	1.3348
O–H	0.15299	1.2798	1.8324	1.16561	1.9370

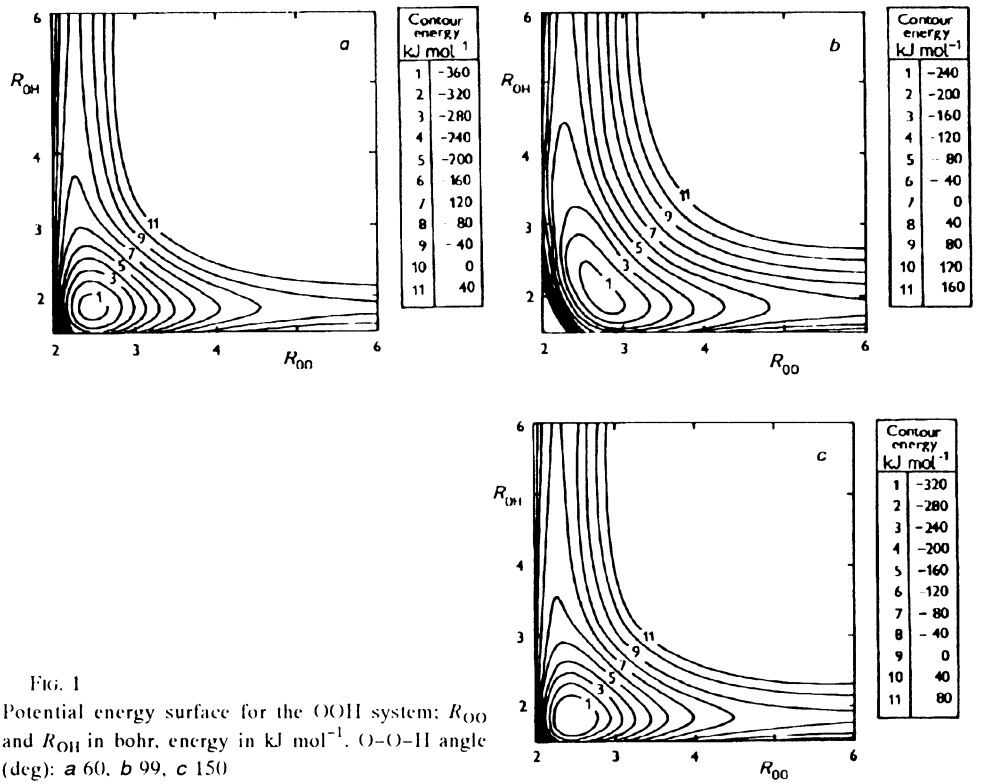

FIG. 1
Potential energy surface for the OOH system; R_{OO} and R_{OH} in bohr, energy in kJ mol^{-1}. O–O–H angle (deg): *a* 60, *b* 99, *c* 150

character of the ELEPS surface is determined by a deep potential energy minimum located in the region of decay of the O–H bond and formation of the O–O bond. The absence of saddle points on the reaction coordinate bears out the fact that the exothermal reaction is fast and at the combustion temperatures, the reaction will only be hindered by the formation of the long-lived OOH complex and its stabilization to the OOH radical.

Dynamic Characteristics

The calculations were based on the standard QCT procedure[29,30] with a constant integration step of $0.15 \cdot 10^{-16}$ s. The beginning of the trajectories was at a distance of the O atom from the OH molecule of $7 \cdot 10^{-10}$ m. The collision energies E of the reactants correspond to the mean relative velocities of the reactant molecules at 500, 1 000, 1 500 and 2 000 K. Also the vibrational quantum number $v = 0$ and the rotational quantum numbers $j = 7, 8, 9$ for the OH molecule were determined as the mean values for the temperature region in question based on the Boltzmann distribution function. The basic QCT data are summarized in Table III. The maximum impact parameter b_{max} decreases with increasing collision energy E and hence, with increasing temperature. On the other hand, it is not visibly dependent on the quantum number j of the OH radical within the regions concerned. Its decrease with increasing translational temperature is consistent with the assumed concept of the OH molecule at higher relative velocities being unable to capture the H atom at distances at which the reaction still occurs at lower velocities. The number of reactive trajectories N_r (out of the total number of trajectories N) decreases with increasing rotational quantum number across the entire region of collision energies (except for $T = 1\,500$ K, $j = 7$). Thus, in this case there predominates the so-called orientation effect, where increasing rotational energy of the OH radical brings about departure from the optimum reaction pathway and subsequent decrease in the number of reactive collisions. The N_r value in dependence on E (for the various j's) exhibits a maximum at 1 000 K, except for the case of $j = 7$. However, the reactivity of the O + OH system, represented by the rate constant and its temperature dependence, is affected by other factors as well, as will be discussed later.

The rotational excitation of the O_2 molecule as a product of reaction (*A*) is most simply characterized by the rotational quantum number j'. To get an idea of how the rotational temperature of O_2 molecules varies with macroscopic temperature T we plotted the $\overline{j'}(T)$ dependence (Fig. 2). The points in this plot (as well as in the $\overline{v'}(T)$ and $\overline{l'}(T)$ plots) were determined by averaging over all j's for $j = 7, 8, 9$ at the collision temperature corresponding to the given temperature and by additional averaging over the above j values using the Boltzmann statistical weights for the given temperature. The results in Fig. 2 point to high rotational temperatures of the O_2 molecule: $\overline{j'}$ lies within the region of 34 – 54 while the mean Boltzmann value of the rotational quantum number is within the region of 15 – 31. The increasing trend of $\overline{j'}(T)$ is related with the

fact that higher rotational states j acquire a higher weight with increasing T, and the $\bar{j}'(j)$ dependence is increasing in the majority of reactive collision processes. Moreover, the increasing trend of the $\bar{j}'(T)$ function is also promoted by the efficient transfer of the translational energy of the reactants to the rotational energy of the products. In conclusion, the O_2 molecules emerging from reaction (*A*) are "hot" within the temperature region concerned; this fact must be taken into account when modelling the hydrocarbon and polymer combustion mechanism. Their rotational temperature will increase with increasing temperature of combustion.

The dependence of the mean vibrational quantum number $\bar{v}'(T)$ for the O_2 molecule (Fig. 3), on the other hand, has a decreasing trend. This means that increase in the macroscopic temperature of the reactants will be accompanied by a decrease in the vibrational temperature of the products of reaction (*A*). This result, which was astonishing at first glance, pointed to the necessity to analyze the v' values. The nature of the effect was found in the decrease in the vibrational numbers with increasing relative translational energy of the reactants. Deeper investigation into this phenomenon brought us to Figs 1*a* – 1*c*, where the repulsive wall (from which the trajectories recoil) gradually departs to the left at a contour line with a higher number. In this manner, increasing translational energy gradually reduces the preconditions for an efficient transformation of the relative translational energy of the reactants into the vibrational energy of the O_2 molecules. The absolute values of $\bar{v}'$ lie within the region of 2.2 – 1.7 while the values of 0.1 – 0.8 correspond to the mean Boltzmann value of the vibrational number of O_2 molecules for the limits of the temperature range. Hence, as in the case of the rotational temperature, also the vibrational temperature of the O_2 molecules emerging from the reaction is higher than as corresponds to the macroscopic temperature of combustion, and this will have a bearing on the consecutive reactions of O_2.

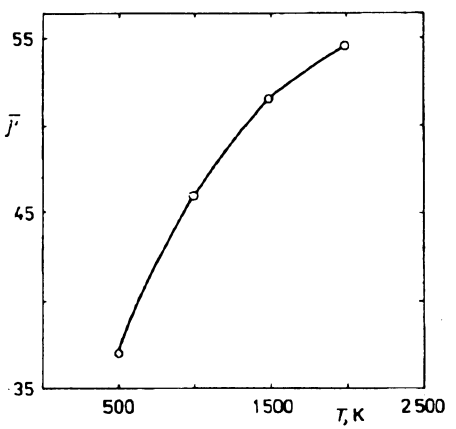

FIG. 2
Dependence of the average rotational quantum number $\bar{j}'$ of the O_2 molecules on temperature T

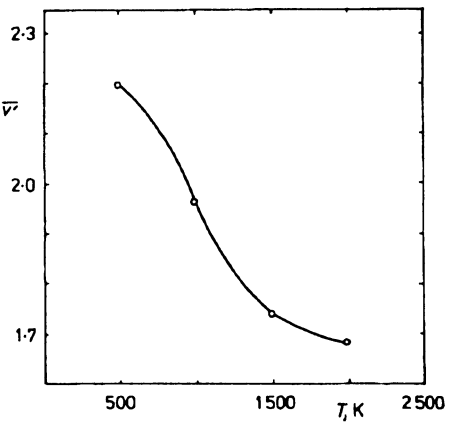

FIG. 3
Dependence of the average vibrational quantum number $\bar{v}'$ of the O_2 molecules on temperature T

In contrast to the rotational temperature, however, the vibrational temperature decreases with increasing T and in the conditions of very high temperatures of combustion of hydrocarbons and polymers it will approach the macroscopic temperature of the burning mixture.

The mean lifetime $\bar{t}$ of the OOH collision complex was determined as the time of existence of such an OOH configuration where each internuclear distance is shorter than $3 \cdot 10^{-10}$ m (ref.[31]). The $\bar{t}(T)$ dependence (Fig. 4) shows the mean lifetime of such an OOH complex which decays to O_2 + H solely. Thus the $\bar{t}$ value has an inversely proportional effect on the rate constant of reaction (*A*). For getting a notion of the absolute value of $\bar{t}$ it should be noted that the vibrational period of the OH molecule ($v = 0$) is $8.92 \cdot 10^{-15}$, so that the OOH complex executes tens of vibrations during its life. The increasing trend of the $\bar{t}(T)$ function is difficult to interpret because the lifetime of the collision complex usually decreases with increasing collision temperature of reactants. In this case, the decrease in the b_{max} values with increasing temperature will apparently play the major role (Table III); owing to this fact, the formation of a more compact collision complex with a longer lifetime is made possible at higher temperatures, which enables the competitive stabilization reaction OOH* + M → OOH + M to manifest itself.

Rate Constant

The reaction cross sections S_r (required to calculate the rate constant) and their dependence on the collision energy were determined based on data in Table III. Figure 5

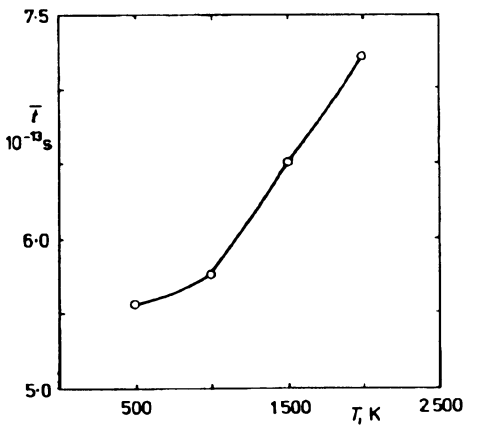

FIG. 4
Dependence of the mean lifetime $\bar{t}$ of the OOH collision complex on temperature T

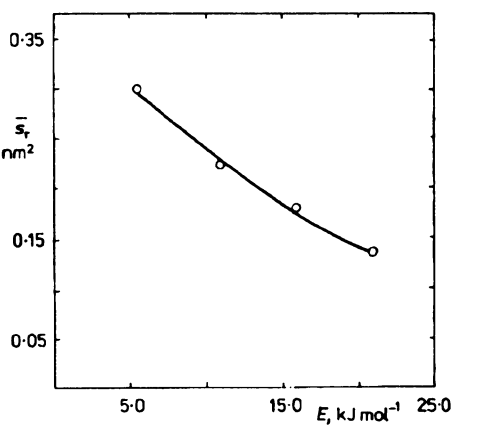

FIG. 5
Dependence of the average reaction cross section $\bar{S}_r$ on the relative translational energy of the O + OH system

shows the dependence of $\bar{S}_r$ on the relative energy E of the O + OH system; the mean $\bar{S}_r$ values were obtained by Boltzmann averaging of the S_r values for the rotational states j = 7, 8, 9. The result is a decreasing $\bar{S}_r(E)$ dependence, which is commonplace for exothermal reactions free of any energy barrier. The rate constant $k(T)$ was calculated from Eq. (3) (e.g. ref.[32]):

$$k(T) = p(T)\,(\pi\mu)^{1/2}\,(2/kT)^{1/2}\int_0^\infty \bar{S}_r(E)\exp(-E/kT)\,E\,\mathrm{d}E\ . \qquad (3)$$

Involved in this relation is the probability of collision initialization $p(T)$ just on the PES studied by us. This parameter has to be considered in cases of degeneration and fine splitting of several PES's in the region of the separate reactants. Since in our case there are involved five degenerate ground states of $O(^3P_2)$, three degenerate excited states of $O(^3P_1)$, one excited state of $O(^3P_0)$, and furthermore two fine split ground states for $OH(^2\Pi_{3/2})$ and two fine split excited states for $OH(^2\Pi_{1/2})$, we used $p(T)$ in the form given and discussed in ref.[10], viz.

$$p(T) = \frac{2}{[5 + 3\exp(-228/T) + \exp(-326/T)]\,[2 + 2\exp(-205/T)]}\ . \qquad (4)$$

The rate constant then can be written as

$$k(T) = p(T)\,k_0(T)\ . \qquad (5)$$

Graff and Wagner[10] also discussed the case where all reactants are at the lowest levels and $p(T)$ = 0.2. In both cases they proceeded from the concept where the reaction can occur at the lowest PES only and nonadiabatic effects are negligible. In the case of the thermal fine structure they obtained a $k(T)$ dependence with a maximum at a temperature lower than 100 K and with a decreasing trend in the region up to 1 000 K. For a

TABLE III
Basic QCT data for reaction (*A*)

T, K	E, kJ mol^{-1}	b_{max}, 10^{-10} m	N_r [a]		
			j = 7	j = 8	j = 9
500	5.29	4.8	232	174	166
1 000	10.59	4.5	206	186	183
1 500	15.88	4.3	169	173	146
2 000	21.17	4.2	156	127	113

[a] N = 500 in all cases.

constant $p(T)$ the rate constant slowly decreases monotonically with temperature. Our data are given in Table IV and compared with the experimental values from refs[13,20] within the temperature regions of measurement. It is evident that the rate constant 0.2 k_0 passes a maximum at approximately 780 K, to decrease at higher temperatures. The decreasing $p(T)$ dependence, however, predominates and governs the decreasing trend of $k(T)$ over the temperature region examined. The experimental data were determined from the temperature dependence of the rate and equilibrium constants of the reverse reaction according to ref.[13]. The very good agreement of the calculated and experimental values gives evidence that the concept of the fine splitting of reactant levels and the temperature dependence of the probability $p(T)$ according to Eq. (*4*) are correct. Moreover, it appears that in spite of its simplicity, the ELEPS surface[28] is able to correctly describe the crucial parts of the potential surface for the QCT calculation of the rate constants.

TABLE IV
Temperature dependence of rate constant k in Eq. (*3*) and its components p and k_0 in Eq. (*5*), and experimental values from refs[13,20] (k and k_0 in 10^{-11} cm^3 molecule^{-1} s^{-1})

T, K	p	k_0 0.2	k	k (ref.[13])	k (ref.[20])
500	0.081	6.06	2.45	–	–
1 000	0.068	6.24	2.12	2.68	2.10
1 500	0.064	5.81	1.85	1.85	1.68
2 000	0.062	5.25	1.62	1.53	1.39

The authors wish to thank their colleague J. Rychlý for valuable remarks on the work and discussions concerning the combustion of hydrocarbons and polymers.

REFERENCES

1. Warnatz J. in: *Rate Coefficients in the C/H/O System in Combustion Chemistry* (W. C. Gardiner, Ed.), p. 197. Springer Verlag, New York 1984.
2. Graff M. M.: Astrophys. J. *339*, 239 (1989).
3. Anderson J. G.: Ann. Rev. Phys. Chem. *39*, 489 (1987).
4. Lazár M., Rychlý J., Klimo V., Pelikán P., Valko L.: *Free Radicals in Chemistry and Biology*. CRC Press, Boca Raton 1989.
5. Quintales L. A. M., Varandas A. J. C., Alvariño J. M.: J. Phys. Chem. *92*, 4552 (1988).
6. Pastrana M. R., Quintales L. A. M., Brandao J., Varandas A. J. C.: J. Phys. Chem. *94*, 8073 (1990).
7. Davidsson J., Nyman G.: J. Chem. Phys. *92*, 2407 (1990).
8. Nyman G., Davidsson J.: J. Chem. Phys. *92*, 2415 (1990).

9. Graff M. M., Wagner A. F.: Chem. Phys. Lett. *174*, 287 (1990).
10. Graff M. M., Wagner A. F.: J. Chem. Phys. *92*, 2423 (1990).
11. Cohen N., Westberg K. R.: J. Phys. Chem., Ref. Data *12*, 531 (1983).
12. Frank P., Just T.: Ber. Bunsenges. Phys. Chem. *181*, 89 (1985).
13. Shin K. S., Michael J. V.: J. Chem. Phys. *95*, 262 (1991).
14. Bamford C. H., Tipper C. F. H.: *Comprehensive Chemical Kinetics, Gas-Phase Combustion*, Vol. 17. Elsevier, Amsterdam 1977.
15. Cullis C. F., Hirschler M. M.: *The Combustion of Organic Polymers*. Clarendon Press, Oxford 1981.
16. Langhoff S. R., Jaffe R. L.: J. Chem. Phys. *71*, 1475 (1979).
17. Melius C. F., Blint R. J.: Chem. Phys. Lett. *64*, 183 (1979).
18. Walch S. P., Rohlfing C. M., Melius C. F., Bauschlicher C. W.: J. Chem. Phys. *88*, 6273 (1988).
19. Varandas A. J. C.: J. Mol. Struct., Teochem *166*, 59 (1988).
20. Yuan T., Wang C., Yu C. L., Frenklach M., Rabinowicz M. J.: J. Phys. Chem. *95*, 1258 (1991).
21. Shepard R. in: *Ab Initio Methods in Quantum Chemistry* (Adv. Chem. Phys. *69*), (K. P. Lawley, Ed.), p. 63. Wiley, New York 1987.
22. Lischka H., Shepard R., Brown F. B., Shavitt I.: Int. J. Quantum Chem., S *15*, 91 (1981).
23. Shepard R., Shavitt I., Pitzer R. M., Comeau D. C., Pepper M., Lischka H., Szalay P. G., Ahlrichs R., Brown F. B., Zhao J. G.: Int. J. Quantum Chem., S *22*, 149 (1988).
24. Dunning T. H.: J. Chem. Phys. *53*, 2823 (1970).
25. Huzinaga S.: J. Chem. Phys. *42*, 1293 (1965).
26. Huber K. P., Herzberg G.: *Molecular Spectra and Molecular Structure*, Vol. IV. Van Nostrand, New York 1979.
27. Ogilvie J. F.: Can. J. Spectrosc. *19*, 171 (1973).
28. Wagner A. F., Schatz G. C., Bowman J. M.: J. Chem. Phys. *74*, 4960 (1981).
29. Truhlar D. G., Muckerman J. T. in: *Atom–Molecule Collision Theory: A Guide for Experimentalists* (R. B. Bernstein, Ed.), p. 505. Plenum Press, New York 1979.
30. Hopper D. G.: *QCPE Program 248*. Indiana University, Bloomington 1974.
31. Sorbie K., Murrell J. N.: Mol. Phys. *31*, 905 (1976).
32. Klimo V., Tiňo J.: *Dynamika elementárnych chemických procesov*. Veda, Bratislava 1991.

Translated by P. Adámek.